

# Future Crop Risk Estimation Due to Drought, Extreme Temperature, Hail, Lightning, and Tornado at the Census Tract Level in Louisiana

Rubayet Bin Mostafiz<sup>1,2,3\*</sup>, Robert V. Rohli<sup>1,2</sup>, Carol J. Friedland<sup>3</sup>, Melanie Gall<sup>4</sup>, Nazla Bushra<sup>1</sup>

<sup>1</sup>Department of Oceanography & Coastal Sciences, Louisiana State University, Baton Rouge, LA, United States

<sup>2</sup>Coastal Studies Institute, Louisiana State University, Baton Rouge, LA, United States

<sup>3</sup>LaHouse Resource Center, Department of Biological and Agricultural Engineering, Louisiana State University Agricultural Center, Baton Rouge, LA, USA

<sup>4</sup>Center for Emergency Management and Homeland Security, Arizona State University, Phoenix, AZ, United States

## \* Correspondence:

Rubayet Bin Mostafiz  
rbinmo1@lsu.edu

**Keywords: weather impacts, natural hazards, crop loss, resilience, Louisiana, risk assessment**

## Abstract

Louisiana is one of the most hazard-prone states in the U.S., and many of its people are engaged directly or indirectly in agricultural activities that are impacted by an array of weather hazards. However, most hazard impact research on agriculture to date, for Louisiana and elsewhere, has focused on floods and hurricanes. This research develops a method of future crop loss risk assessment due to droughts, extreme low and high temperatures, hail, lightning, and tornadoes, using Louisiana as a case study. This approach improves future crop risk assessment by incorporating historical crop loss, historical and modeled future hazard intensity, cropland extent, population, consumer demand, cropping intensity, and technological development as predictors of future risk. The majority of crop activities occurred and will continue to occur in south-central and northeastern Louisiana along the river basins. Despite the fact that cropland is decreasing across most of the state, weather impacts to cropland are anticipated to increase substantially by 2050. Drought is by far the costliest among the six hazards, accounting for \$56.1 million of \$59.2 million (~95%) in 2050-projected crop loss, followed by extreme cold (\$1.4 million), extreme heat (\$1.0 million), tornadoes (\$0.4 million), hail (\$0.2 million), and lightning (\$0.05 million), respectively. These findings will assist decision-makers to minimize risk and enhance agricultural resilience to future weather hazards, thereby strengthening this economically-important industry in Louisiana and enhancing food security.

## 41 Introduction

Increases in population and development bring a sharp increase in the risk (i.e., the product of the probability of a hazardous event and the consequences of that event) associated with weather hazards (Bushra et al. 2021). This risk is exacerbated by policy that incentivizes development without considering the additional complications in mitigating risk to the increasing hazard exposure. The encouragement of additional development only further increases vulnerability and reduces resilience to the hazard in a positive feedback mechanism. Ultimately, environmental, social, and economic sustainability become impractical unless compensating action is taken.

While loss and risk occur in a wide range of ways, much weather hazard research focuses on property damage (e.g., Mostafiz et al. 2020a, 2021a, 2021b, 2021c, 2021d, [2022a](#)) and casualties (e.g., Jonkman 2005). Although such research is beneficial, the risk posed to agriculture is often ignored. Moreover, the risk to agriculture posed by less-catastrophic weather hazards such as those due to lightning (e.g., Zhang et al. 2011), hail (e.g., Changnon 1972), mid-latitude wave cyclones (e.g., Mukherjee et al. 2018), and other weather hazards is also important and understudied, even as underutilized data sources, including comprehensive historical loss databases and sophisticated model output to estimate the changing hazard intensities, exist to improve such future risk assessments ([Mostafiz 2022c](#)). Assessing weather hazard risk to agriculture precisely and accurately, especially in spatially heterogeneous areas, is also often problematic due to a coarse scale of analysis. Another complication is that future population and/or land cover changes ~~confound~~[confound](#)~~implicate~~ projection of the future risk to agriculture.

The purpose of this research is to address these gaps by developing a geospatially-based risk assessment method for census-tract-level future crop loss due to drought, extreme cold and hot temperatures, hail, lightning, and tornadoes, using Louisiana, one of the most weather-vulnerable U.S. states, as a case study.

## 52 Background

Geospatial approaches to understanding the changing weather hazard risk have proliferated in recent years. For example, Kebede and Nicholls (2012) showed that flood exposure increases are a function of the spatial distribution of socio-economic variables (i.e., economic development, urbanization, and population growth). In an analysis of socio-economic factors contributing to natural hazard exposure at the U.S. county-scale, Preston (2013) found that despite disaster risk management successes, the U.S. continues to face dire consequences of increasing economic losses due to extreme weather events. The first Intergovernmental Panel on Climate Change (IPCC) report (Cutter et al. 2012) confirmed these assertions by reporting that societal exposure (and therefore risk as defined here) is a product of development processes on hazardous landscapes and also is an anticipated key driving force contributing to future vulnerability to extreme weather events (Pielke et al. 2007; Hinkel et al. 2010). There remains a paucity of risk assessment work at a scale more local than county-level, especially while also considering changing hazard intensities ([Gnan et al. 2022a; 2022b, Mostafiz et al. 2022b; 2022d, Rahim et al. 2022](#)).

Several recent studies have focused on risk assessment and/or exposure/loss due to drought (e.g., Bushra et al. 2019). Wilhite (2000) noted that drought and agricultural losses in general stand out among weather hazards in terms of risk and exposure, and both are increasing sharply, and lamented the long-problematic lack of reliable, accurate, and accessible historic loss data. More recently, drought monitoring and crop loss prediction has improved with the Visible Infrared Imaging Radiometer Suite (VIIRS) sensor in the National Oceanic and Atmospheric Administration (NOAA) Suomi National Polar-Orbiting Partnership (S-NPP) satellite, which was launched in 2011 (Kogan et al. 2015). Numerous studies suggest that crop growing cycle exposure to drought and other hazards, including extreme temperatures and hail, is increasing with time (Potopova et al. 2016) and is likely to continue increasing, resulting in decreasing crop yields (Guo et al. 2017; Leng and Hall 2019), though benefits of CO<sub>2</sub> fertilization and adaptations may be underestimated. Analyses at shorter time scales improve efforts to identify drought impacts on crop yields (Peña-Gallardo et al. 2019). Many of these themes are echoed in the fourth (U.S.) National Climate Assessment (NCA4) from the U.S. Global Change Research Program (USGCRP; Gowda et al. 2018).

Similarly, several recent studies have focused on projecting future risk due to extreme temperatures. Forzieri et al. (2017) concluded that European weather-related risk in 2100 due to cold, heat waves, and other hazards has increased 50-fold over the 1981–2010 period due to the increase in population exposed amid global warming. Zhang and Hu (2018) studied risk assessment of extreme cold temperature events in China using a copula distribution model based on intensity and duration of the hazard. In a crop-focused extreme temperature risk assessment, Annan and Schlenker (2015) found that in the U.S., insured soybeans and corn have 43 and 67 percent more sensitivity, respectively, to extreme heat than uninsured crops, and extreme heat is well-understood to decrease crop yields in Georgia and the Carolinas (Eck et al. 2020). Some (e.g., Lesk et al. 2016) have explained that extreme cold is less impactful than extreme heat, because cold temperatures usually occur outside of the normal growing season. In addition, if the warming temperatures occur uniformly across the seasonal cycle, extreme low temperatures will become less frequent. However, others (e.g., Gu et al. 2008) have suggested that the opposite net effect may occur – that rising temperatures may cause increased vulnerability to cold by inducing premature budding and growth before a subsequent unseasonable cold outbreak.

Overall future crop loss due to hail has not been considered comprehensively, yet improved understanding of such losses is economically important, as crop loss due to hail averages approximately 1 percent of the U.S. national annual crop output (Changnon 1972). Leigh and Kuhnel (2001) modeled loss and risk assessment associated with hail for the Sydney, Australia, region, for insurance purposes. Zhou et al. (2016) assessed the hail damage to potatoes in Washington using aerial multispectral imagery at different growth stages and seasons. Wang et al. (2016) found that hail risk increased (1950–2009) in China at different growing stages of cotton in their county-level GIS-based spatiotemporal study. Púčik et al. (2019) noted that crop loss probability increases when the hail size exceeds 2–3 cm, for central Europe.

Lightning impacts are generally considered to be decreasing vis-à-vis death rate (Mills 2020), but this trend is presumably driven by increased awareness facilitated by technological development, with the risk of injuries and crop and property loss still present. While much research has been invested in identifying lightning risk and its impact on property loss (e.g., Brooks et al. 2020; He et al. 2020; Mostafiz et al. 2020b; Villamil et al. 2015), little research focuses on the lightning-induced risk to crop loss. Kocur-Bera (2018) identified the most sensitive places in Poland to damage from lightning, in addition to drought, cold temperatures, hail, and other hazards, but the short (2010–2014) period of record limits conclusions.

Changnon et al. (2001) suggested that from 1950 to 1997, normalized tornado crop losses in the U.S. displayed no temporal trend. Subsequent work on tornado-driven risk assessments has been conducted for losses to nuclear plants (Reinhold & Ellingwood 1982) and property (Mostafiz et al. 2020b; Refan et al. 2020), and generalized tornado-induced losses have been conducted at the community (Masoomi & van de Lindt 2018), and local scales. While not tornadic in nature, the 2020 Iowa derecho (Hosseini et al. 2020) poignantly demonstrates the tremendous crop damage that can result from severe weather in general. However, a need remains for comprehensive analysis of future tornado risk focused on crop loss.

Regardless of whether the hazard examined is drought, extreme temperatures, hail, lightning, or tornadoes, increasing evidence (e.g., Rahman & Rahman 2015) suggests that a comprehensive management plan in at-risk areas, guided by both traditional and scientific considerations, is vital for assessing risk, enhancing resilience, and progressing toward sustainability. Climate change complicates efforts to improve management strategies and makes the future risk due to these hazards even more uncertain. In projecting the probable economic risk for extreme weather events at various return periods under IPCC scenarios, Franzke and Czipryna (2020) found that the risks can be increased by 3-to-5.4-fold for the U.S. by 2060. Such future risk assessments must incorporate methods for projecting population growth accurately (Wu et al. 2018).

Some attempts have been made to quantify resilience that would be useful for agriculture, such as Lam et al. (2016, 2018), who introduced the resilience inference measurement (RIM) approach. While methods such as the RIM model are useful for quantifying resilience, a similarly appropriate means of assessing the risk remains elusive. This is problematic because risk must be evaluated accurately and precisely at the planning stage for development.

In this study, it is hypothesized that, despite a temporally decreasing land cover in crops in Louisiana (Table 1), crop loss from these hazards will increase by 2050 (Gowda et al. 2018) as additional crop yield (Table 2) and production (Table 3) escalate the risk, primarily driven by the increasing population, consumer demand, and exposure to the hazards due to climate change. Enhanced data and methodological techniques are employed to improve the estimation of crop loss risk to these hazards and thereby enhance the likelihood of improved planning for mitigation, adaptation, and resilience.

Table 1. Total cropland in Louisiana (Source: U.S. Department of Agriculture (USDA) National Agricultural Statistics Service (NASS) 2020).

Year	Total Cropland (Acres)
1997	5,567,627
2002	5,071,537
2007	4,691,344
2012	4,275,637
2017	4,345,843

Table 2. Yields of the top five Louisiana crops by value (source: USDA NASS 2020).

Year	Soybeans (bushels/acre)	Corn (bushels/acre)	Rice (pounds/acre)	Cotton (pounds/acre)	Hay (tons/acre)
1949	15	20	1,825	329	1.29
1959	23.5	31	2,850	476	1.45
1969	20.5	37	3,500	551	1.82
1979	28	54	3,910	712	2.21
1989	22	95	4,430	672	2.6
1999	27	121	5,000	709	2.4
2009	39	132	6,300	745	2.8
2019	48	165	6,380	1,035	2.5

Table 3. As in Table 2, but for total production (source: USDA NASS 2020).

Year	Soybeans (1,000 bushels)	Corn (1,000 bushels)	Rice (1,000 cwt)	Cotton (1,000 bales)	Hay (1,000 tons)
1949	345	14,540	10,822	651	395
1959	4,536	12,183	12,910	491	554
1969	32,964	4,477	21,385	482	647

1979	93,800	2,214	20,643	690	849
1989	38,500	13,490	21,488	868	781
1999	26,730	39,930	30,825	901	912
2009	36,660	80,520	29,217	349	1,064
2019	41,280	89,925	26,408	582	975

Drought, extreme cold, extreme heat, hail, lightning, and tornadoes are selected for analysis here because, with some notable exceptions (e.g., Smith & Katz 2013; Smith & Matthews 2015) they are understudied, significant, crop-damage-producers statewide, and are important for Louisiana's State Hazard Mitigation Plan (SHMP). Moreover, with the exception of drought, crop losses due to these hazards can be assessed relatively easily using existing data sources, in contrast to more catastrophic hazards (e.g., floods and hurricanes) in which crop damage occurs from multiple sources (i.e., wind, lightning, tornadoes, etc.) simultaneously but is not partitioned by hazard.

179 6

180 **73 Study Area**

181 The U.S. state of Louisiana is highly vulnerable to extreme weather events both in terms of physical  
 182 exposure as well as in terms of economic and human impacts, given the concentration of people and  
 183 assets in high-risk areas, especially along the Gulf of Mexico (Mostafiz et al. 2021a). Catastrophic  
 184 loss events causing more than \$1 billion in damage are frequent. Since 1980 alone, Louisiana has  
 185 been impacted by 25 severe storms, 19 tropical cyclones, 12 droughts, 9 floods, 7 winter storms, and  
 186 1 freeze—each causing over \$1 billion (2020 Consumer Price Index (CPI) adjustment) in economic  
 187 damage (NOAA National Centers for Environmental Information (NCEI, formerly known as the  
 188 National Climatic Data Center (NCDC), 2020). The Southern Plains/Southwest drought and heat  
 189 wave of spring-summer 2011 cost \$14.2 billion (2020 CPI adjusted) and caused 95 deaths in  
 190 Arizona, Kansas, Louisiana, New Mexico, Oklahoma, and Texas (NOAA NCEI 2020). This drought  
 191 spanned 107 consecutive weeks and is arguably the longest to hit Louisiana, from 04/20/2010 to  
 192 05/01/2012, with approximately 65 percent of Louisiana land cover suffering from exceptional  
 193 drought (D4) in late June 2011 (U.S. Drought Portal 2020). The southeastern U.S. winter storm of  
 194 January 2000 caused four deaths and \$1.1 billion in damage over numerous states, including  
 195 Louisiana. Severe weather, including high winds, hail, and tornadoes, caused \$1.4 billion in damage  
 196 across several southern states including Louisiana in April 2020 (NOAA NCEI 2020). With  
 197 agriculture contributing over \$3.1 billion, or 2.9 percent of the state's gross domestic product  
 198 (University of Arkansas Division of Agriculture 2021), the vulnerability of Louisiana agriculture to  
 199 weather hazards is substantial, including to the leading crops featured in Tables 2 and 3.

200 **84 Data**

201 Crop loss data (1960–2019) at the parish level by hazard type originates from the Spatial Hazards  
 202 Events and Losses Database for the United States (SHELDUS®; Center for Emergency Management  
 203 and Homeland Security (CEMHS) 2020), which collects its data from the NCEI Storm Events  
 204 reports. According to NOAA NCEI (2018, p. 14), “crop damage information may be obtained from  
 205 reliable sources, such as the U.S. Department of Agriculture (USDA), the county (i.e., parish in  
 206 Louisiana) agricultural extension agent, the state department of agriculture, crop insurance agencies,  
 207 or any other reliable authority. Crop damage amounts may be obtained from the USDA or other  
 208 similar agencies.” It should be noted that for Louisiana, drought-induced crop damage was only  
 209 reported and available to SHELDUS beginning in 1996.

210 Because the intended purpose of vegetation determines whether its loss is considered as crop damage  
 211 or property damage (NOAA 2018), this analysis excludes timber, as forested land cover is assumed  
 212 to be unharvested and/or property rather than crop. By contrast, pasture is considered as cropland  
 213 because its intended purpose is assumed to be consumed, although loss of the animals that consume  
 214 the pasture are not considered as crop loss here, but would instead be considered as property loss.  
 215 Moreover, because SHELDUS does not itemize losses by crop, a “bulk” analysis of all crops is  
 216 undertaken here. Annual crop loss in SHELDUS are adjusted to 2019\$. The indicators of historical  
 217 hazard severity and their data sources are shown in Table 4.

218

219

220

221  
222  
|



Table 4. Indicator of hazard severity, data source, and years analyzed, by hazard in Louisiana.

Hazard	Indicator of Hazard Severity	Data Source	Years Analyzed
Drought	Weekly drought intensity	U.S. Drought Monitor	2000–2017
Extreme Cold	Annual frequency of days with temperatures < 32°F	National Centers for Environmental Information (NCEI)	1992–2017
Extreme Heat	Annual frequency of days with temperatures > 95°F	NCEI	1992–2017
Hail	Hail days per year	National Severe Storms Laboratory (NSSL), University of Oklahoma	1982–2011
Lightning	Lightning density per year	NCEI	1986–2012
Tornado	Tornado days per year	Storm Prediction Center (SPC)	1950–2016

Because risk is a product of the probability and consequence of the hazard occurrence, and the latter is a function of the cropland value, the hazard intensity data must be accompanied by data on historical and future cropland extent, demand, and population (which impacts demand). For this reason, Louisiana historical land cover data for 2001, 2003, 2006, 2008, 2011, 2013, and 2016 were downloaded from the National Land Cover Database (NLCD) archived by U.S. Geological Survey (USGS; 2016). Rasters containing the only two categories for crops in the NLCD classification system (pasture/hay (category 81) and cultivated crops (category 82)) comprise the cropland cover data, from the NLCD database. Louisiana crop market values available every five years from 2002 to 2017 from U.S. Department of Agriculture (USDA) National Agricultural Statistics Service (NASS; 2020) and crop export values available annually (2002–2017) from USDA Economic Research Service (2017) were used as indicator of crop demand. Historical and 2050-projected population data for the world and U.S. were acquired from the U.S. Census Bureau (2020) to assess population growth for projecting that demand to 2050. Louisiana census-tract shapefiles were downloaded from the U.S. Census Bureau (2016). The census tract is the best geographic scale to represent the crop land cover and crop loss because census blocks and block groups are too localized (e.g., < 0.01 mi<sup>2</sup>), while parishes and the state level are too coarse to provide an effective representation for cropland to represent individual crops.

## 5 Methods

Because the methodology involves many steps, a flowchart (Figure 1) is used to provide guidance on each step, described in detail in the subsections below.

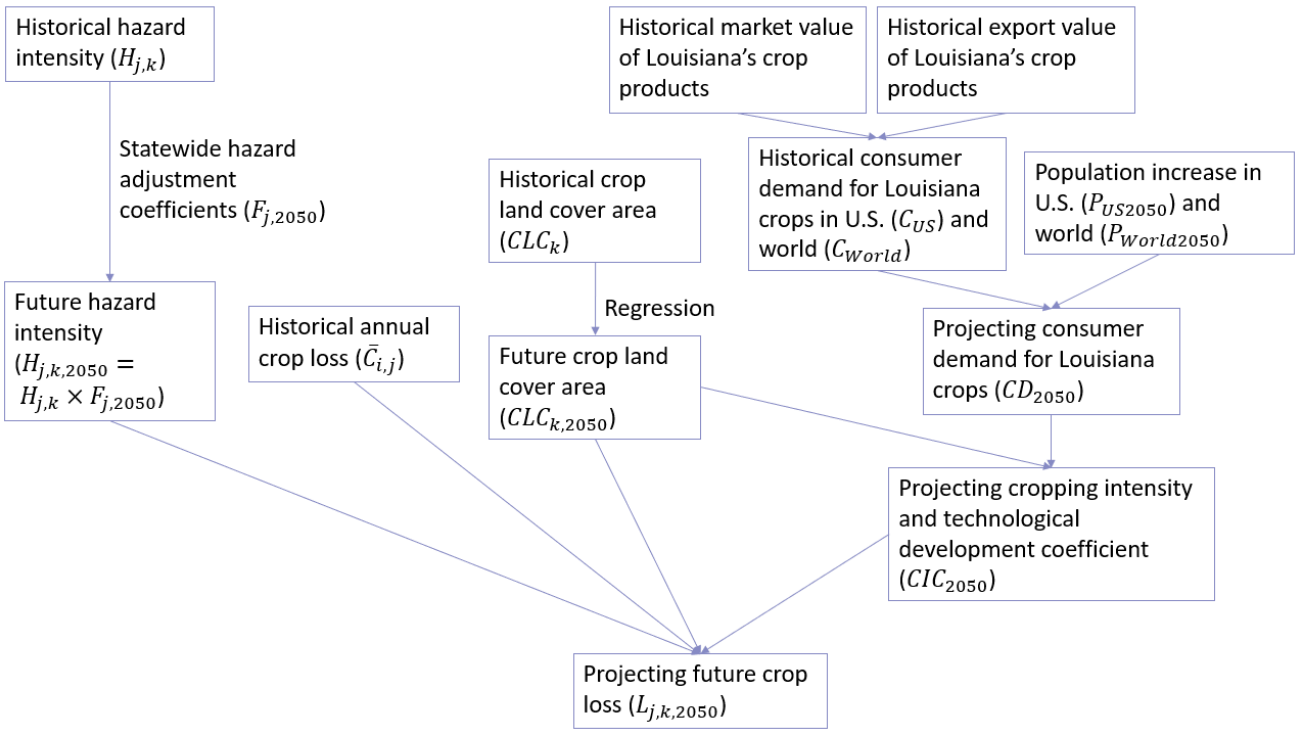


Figure 1. Methodological framework.

8.15.1 Historical Hazard Intensity

For each week, shapefiles of drought intensity from the U.S. Drought Monitor (2017), coded according to the first two columns in Table 5, were rasterized using the value in the second column of Table 5, with a pixel size of 0.0005 x 0.0005 decimal degrees. The drought value for each raster cell was averaged across all weeks (2000–2017), providing the mean weekly historical drought intensity by cell.

255

256 Table 5. Pixel values in drought intensity calculation.

Category	Value for Drought Intensity Analysis
D0 (Abnormally Dry)	0
D1 (Moderate Drought)	1
D2 (Severe Drought)	2
D3 (Extreme Drought)	3
D4 (Exceptional Drought)	4
Normal or Wet Conditions	No value

257 In the extreme cold and high temperature analysis, for 139 stations within and adjacent to Louisiana  
 258 (1/1/1992 to 10/14/2017), any daily data that were missing, erroneous (e.g., minimum temperature  
 259 exceeds maximum temperature on that day), or spurious (following Global Historical Climate  
 260 Network-Daily (NOAA NCEI 2017a)) criteria, were discarded. Furthermore, any station with  
 261 discarded temperature data exceeding 10 percent of days were removed, as were stations with less  
 262 than five years of data. These criteria narrowed the analysis to 102 stations. The mean annual  
 263 frequency of days having temperatures below 32°F, and in a separate analysis, above 95°F, were  
 264 mapped using “ordinary kriging” with a spherical semivariogram, cell size of  $0.0005 \times 0.0005$   
 265 degrees, and variable search radius of 12 points.

266 Methods for analyzing intensity of the other three hazards were relatively straightforward. A map of  
 267 mean annual (1982–2011) frequency of days with hail of 0.75+ inches in diameter within 25 miles  
 268 (NOAA National Severe Storms Laboratory 2014) was digitized. Then, a triangulated irregular  
 269 network (TIN), with these hail-day contour lines generated as hard edge, was developed. This TIN  
 270 was then rasterized using linear interpolation at a cell size of  $0.005 \times 0.005$  degrees. Mean annual  
 271 lightning strike data (1986–2012) were acquired in netCDF format from NOAA NCEI (2017b).  
 272 These data were rasterized to 4 km x 4 km cells and converted using lightning density in flashes mi-2  
 273 yr-1. Tornado touchdown point data (1950–2016) were acquired from the U.S. Storm Prediction  
 274 Center (SPC; 2017). These data were then processed to calculate the mean annual frequency of days  
 275 having a touchdown within 40 km, at a 100 m x 100 m cell size, using a spatial probability density  
 276 heat map derived from kernel density estimation (Epanechnikov 1969) in QGIS®. Further details  
 277 regarding the methodology employed in assessing historical hazard intensity for extreme cold, hail,  
 278 lightning, and tornado are described in Mostafiz et al. (2020b).

279 For each hazard  $j$ , where  $j$  is 1 through 6, the mean historical hazard intensity by census tract  $k$ , where  
 280  $k$  is 1 through 1148 ( $H_{j,k}$ ), was calculated.  $H_{j,k}$  is one of the key factors used for calculating  
 281 projected crop loss by 2050.

## 282 **8.25.2 Future Hazard Intensity**

283 A distinctive feature of our method is the use of statewide adjustment coefficients to represent hazard  
 284 intensity in future year  $x$ ; this produced  $H_{j,x}$  of all six hazards taken individually. Because hazard

frequencies and/or magnitudes may change in the future, statewide adjustment coefficients for hazard  $j$  in future year  $x$  ( $F_{j,x}$ ) were computed considering NCA4-projected (USGCRP 2017) changes to the hazard. Future hazard intensity was then projected in each census tract  $k$  ( $H_{j,k,x}$ ) by modifying historical hazard intensities  $H_{j,k}$  using the statewide adjustment coefficients  $F_{j,x}$  (Equation 1).

$$H_{j,k,x} = H_{j,k} \times F_{j,x} \quad (1)$$

It was then necessary to determine the values of  $F_{j,x}$ . For drought, although Louisiana precipitation is expected to change little by 2100 (Easterling et al. 2017, their Figure 7.5), enhanced evapotranspiration caused by increased temperatures may result in drying soils by 2100 over much of the continental U.S., including Louisiana, at least under the higher radiative forcing and emissions scenario (Wehner et al. 2017; their Figure 8.1). These changes will impact soil moisture availability in Louisiana. Specifically, in Louisiana, winter, spring, and summer soil moisture decreases, made with a “medium” degree of confidence, are projected to be large relative to natural variability (Wehner et al. 2017). For these reasons, an increase in drought hazard of 25 percent was assumed for the state by 2050, or  $F_{drought,2050} = 1.25$ .

Similarly,  $F_{j,x}$  for extreme heat was considered to increase by 20 percent ( $F_{extreme\ heat,2050} = 1.20$ ), based on data in NCA4 by Vose et al. (2017; their Figure 6.9), although their figure used 90°F as the threshold rather than the 95°F used in the historical analysis here. As described in Mostafiz et al. (2020b), changes to the extreme cold temperature hazard were assumed to parallel the projected changes to the annual mean frequency of sub-0°C days. Vose et al. (2017; their Figure 6.9) also estimated such changes. Thus,  $F_{j,x}$  for extreme cold temperature was assumed to decrease by 20 percent by 2050 ( $F_{extreme\ cold,2050} = 0.80$ ).

An analogous method of representing the severe storm (hail, lightning, and tornado) hazards as that presented in Mostafiz et al. (2020b) was employed here. Specifically, the method of assigning  $F_{j,x}$  was determined by weighing the results of current modeling-based literature. One line of theoretical consideration suggests that the frequency and/or intensity of severe thunderstorms in Louisiana capable of producing hail and lightning may decrease. This is because the expected increasing temperatures through at least 2050 would shift the cold/warm air mass interface and associated polar front jet stream poleward, leaving Louisiana less frequently near the peak area for tornadic development (i.e., along vigorous cold fronts trailing from mid-latitude wave cyclones). The increasing temperatures would also decrease the frequency/intensity of hail events because the percentage of time and vertical extent that subfreezing temperatures exist in the cumulonimbus clouds that produce hail would decrease with increasing temperatures. The seasonality of the magnitudes of projected warming is likely to be less important for this analysis than it might be for most other locations, because severe thunderstorms and tornadoes show less seasonality in Louisiana than in most other places.

However, other factors suggest increasing frequency/intensity of future hail- and lightning-producing thunderstorms and tornadoes. Thunderstorm and tornadic activity is most likely when energetic, near-surface air underlies much colder air, so the continued surface warming would destabilize the atmosphere, tending toward a net enhancement of severe storm activity. Brooks (2013) concluded that the vertical temperature gradient, or instability, as represented by a severe weather index known

as convective available potential energy (CAPE, measured in  $\text{J kg}^{-1}$ ), is expected to increase. However, Brooks (2013) also noted the compensating effect of expected weakening of the vertical wind shear that spawns tornadoes. Gensini et al. (2014) suggested that atmospheric instability (as represented by frequency of days with abundant CAPE) is likely to weaken over nearly all of Louisiana, for the 2041–2065 period vs. 1981–1995. Collectively, this research guides our assignment of  $F_{j,x}$  of a 10 percent decrease for hail, and a 10 percent increase for lightning and tornadoes by 2050 compared to the present ( $F_{\text{hail},2050} = 0.90$ ;  $F_{\text{lightning},2050} = 1.10$ ;  $F_{\text{tornado},2050} = 1.10$ ). Of course, different hazard intensities would be derived for similar analyses for projections of years other than 2050.

For each hazard, a sensitivity analysis is run, to produce loss estimates for 2050 assuming an over- or under-estimation by 10 percentage points. For example, the 25 percent increase in the drought hazard would mean that the sensitivity analysis is run assuming values of 1.15, 1.25, and 1.35 for  $F_{j,x}$ .

### 8.35.3 Quantifying Historical Annual Crop Loss and Projecting Crop Land Cover Change

SHELDUS-based historical, inflation-adjusted (to represent 2019\$) crop loss by parish ( $i$ ) was aggregated to annual total by hazard ( $j$ ) and used to represent the economic impacts of past events. For each  $i$  and  $j$ , mean annual crop loss,  $\bar{C}_{i,j}$  was computed as the mean historical annual crop loss (2019\$) for the 60-year period from 1960 to 2019 (excepting drought, for which, as explained earlier, crop loss was available for Louisiana only since 1996), as depicted in Equation 2.

$$\bar{C}_{i,j} = \frac{[C_{i,j,1960} + C_{i,j,1961} + C_{i,j,1962} + \cdots + C_{i,j,2018} + C_{i,j,2019}]}{60} \quad (2)$$

The crop land cover area (CLC) from NLCD (including pasture and hay) of each census tract ( $k$ ) was calculated for the available years (2001, 2004, 2006, 2008, 2011, 2013, and 2016;  $CLC_k$ ). The  $CLC_k$  for 2050 was then projected by fitting a regression line through the historical land cover area. Each  $CLC_k$  for 2050 was verified to fall between zero and the census tract area. The data and regression parameters for three example census tracts ( $k$ ) are shown in Table 6.

Table 6. Examples regression-based projection of crop land cover area ( $\text{km}^2$ ) by 2050 by census tract ( $CLC_{k,2050}$ ).

Census Tract	2001	2004	2006	2008	2011	2013	2016	Intercept	Slope	2050
22001960300	124.1	123.9	123.3	123.3	122.9	122.9	122.7	318.8	(0.10)	119.3
22003950400	129.3	126.9	124.6	121.5	119.9	120.4	120.4	1,415.9	(0.64)	96.5
22005030102	6.1	6.1	5.8	5.8	5.8	5.8	5.7	62.7	(0.03)	4.7

### 8.55.4 Projecting Consumer Demand for Louisiana Crops

A method of estimating future consumer demand of those crops based on trends historical and current consumption (i.e., domestic vs. international) and future population projections was necessary.

Specifically, the percentage of domestic vs. international consumption was calculated from the mean historical market value (Table 7) and export value (Table 8) of Louisiana's crop-based products. Tables 7 and 8 suggest that 58.5 percent of Louisiana crops is exported (i.e., consumed

Table 7. Total market value of crop products in Louisiana (USDA NASS 2020).

Year	Market Value of Crop (\$ million)
2017	2,061
2012	2,784
2007	1,605
2002	1,066
Mean	1,879

Table 8. Total export value of crop products in Louisiana (USDA Economic Research Service 2017).

Year	Export Value of Crop Products (\$ million)
2017	1259
2016	1133
2015	1350
2014	1604
2013	1614
2012	1653
2011	1439
2010	1253
2009	982
2008	1069
2007	985
2006	711
2005	664
2004	703
2003	688
2002	495
Mean	1100

internationally,  $C_{World}$  or 0.585), and therefore, 41.5 percent is consumed domestically ( $C_{U.S.}$  or 0.415). U.S. Census Bureau (2020) estimates that U.S. population will increase by 16.9 percent by 2050 ( $P_{US2050}$ ) and world population is estimated to increase by 26.4 percent ( $P_{world2050}$ ). Assuming no changes in consumer demands, competition, innovation, and consumption patterns, the consumer demand increase coefficient of Louisiana crops for 2050 ( $CD_{2050}$ ) was computed as a weighted average, or as

$$CD_{2050} = 1 + (C_{World} \times P_{World2050} + C_{US} \times P_{US2050}) = 1.225 \quad (3)$$

Thus, assuming that the production will meet this demand, an additional 22.5 percent of crop value (2019\$) will be exposed to hazards by 2050.

### 8.65.5 Projecting Cropping Intensity and Technological Development Coefficient

It was assumed that technological development will increase agricultural efficiency, as for global trends (Foley et al. 2011), to meet the increasing  $CD_{2050}$  for Louisiana's crops, despite the NLCD-regression-projected 9.5 percent decrease in Louisiana's areal cropland from 2016 to 2050. Thus, the projected crop land cover coefficient in 2050 ( $CL_{2050}$ ) is the quotient of 100 divided by  $(100 - 9.5)$ , or 1.105. The future cropping intensity and technological development coefficient for 2050 ( $CIC_{2050}$ ) was estimated simply as

$$CIC_{2050} = CD_{2050} \times CL_{2050} = 1.225 \times 1.105 = 1.354 \quad (4)$$

This approach assumes that consumer demand increase and crop land cover decrease contribute equally toward the intensity/technological development coefficient.

### 8.75.6 Projecting Future Crop Loss

Because overall crop loss is impacted by both the presence and intensity of the hazard acting on the crop land cover in a given census tract, a method of representing each is important. For each hazard (analyzed separately), the parish-level, hazard-and-cropland-adjusted loss ratio  $LR_{i,j,2016}$  was calculated by dividing the mean annual historical parish-level crop loss ( $\bar{C}_{i,j}$ , from SHEL DUS) by the product of historical hazard intensity ( $H_{j,k}$ ) and baseline 2016 crop land cover area ( $CLC_{k,2016}$ ) for each census tract within that parish ( $n$ ), or

$$LR_{i,j,2016} = \frac{\bar{C}_{i,j}}{\sum_{k=1}^n (H_{j,k} \times CLC_{k,2016})} \quad (5)$$

This method assigns the total historical parish loss based on the sum of the product of these factors.

To estimate census-tract-level crop loss by hazard in 2050 ( $L_{j,k,2050}$ ),  $LR_{i,j,2016}$  from Equation 5 is applied to the future mean annual hazard intensity ( $H_{j,k,2050}$ ; from Equation 2), future cropping



intensity and technological development coefficient ( $CIC_{2050}$ ; from Equation 4), and crop land cover area ( $CLC_{j,2050}$ ; as calculated by the example in Table 6) within the census tract, or

$$L_{j,k,2050} = LR_{i,k,2016} \times H_{j,k,2050} \times CIC_{2050} \times CLC_{j,2050} \tag{6}$$

96 Results and Discussion

9.16.1 Historical and Future Hazard Intensity

Historical hazard intensity ( $H_j$ ) for each hazard is mapped in Figure 4A2A-F. The northwestern part of Louisiana is the most vulnerable section of the state to drought, extreme heat, and hail (Figures 4A2A, 4E2C, and 4D2D, respectively). Not surprisingly, extreme cold temperatures are most common throughout northern Louisiana (Figure 4B2B). Lightning density is concentrated in urban areas, particularly in the southeast (Figure 4E2E). Tornado intensity peaks prominently in south-central Louisiana, with a secondary area of maximum intensity in northwestern Louisiana (Figure 4F2F).

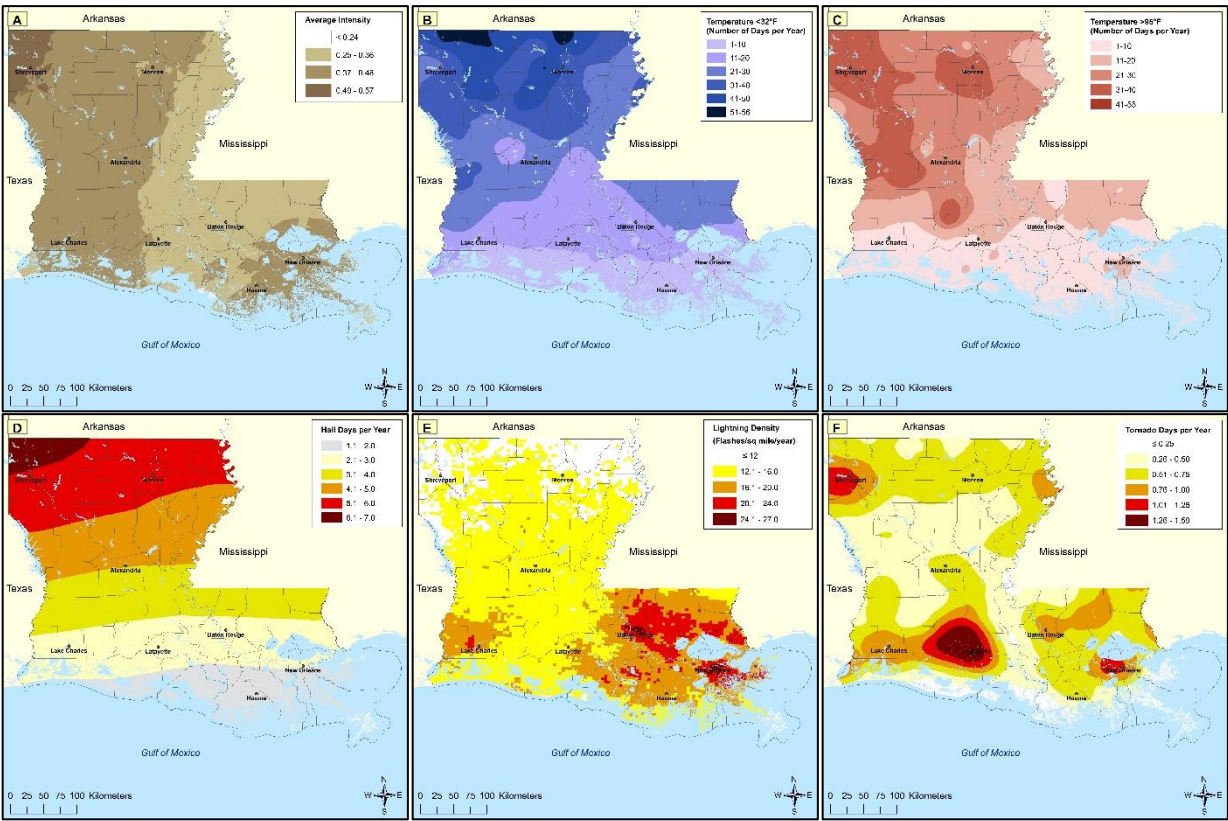


Figure 42. Historical mean hazard intensity ( $H_j$ ) in Louisiana: A) drought (2000–2017), B) extreme cold temperature (1992–2017; Mostafiz et al. 2020b), C) extreme heat (1992–2017), D) hail (1982–2011; Mostafiz et al. 2020b), E) lightning (1986–2012; Mostafiz et al. 2020b), and F) tornado (1950–2016; Mostafiz et al. 2020b).

Projected changes to the hazard intensities ( $H_{j,2050}$ ) by 2050 are shown in Figure 2A3A-F. Decreases in the extreme cold temperature and hail frequencies are apparent by comparing Figures 4B2B to 2B



3B and 4D-2D to 2D3D, respectively. The lightning-intensity hazard is projected to increase for southeastern Louisiana (compare Figure 4E-2E to 2E3E).

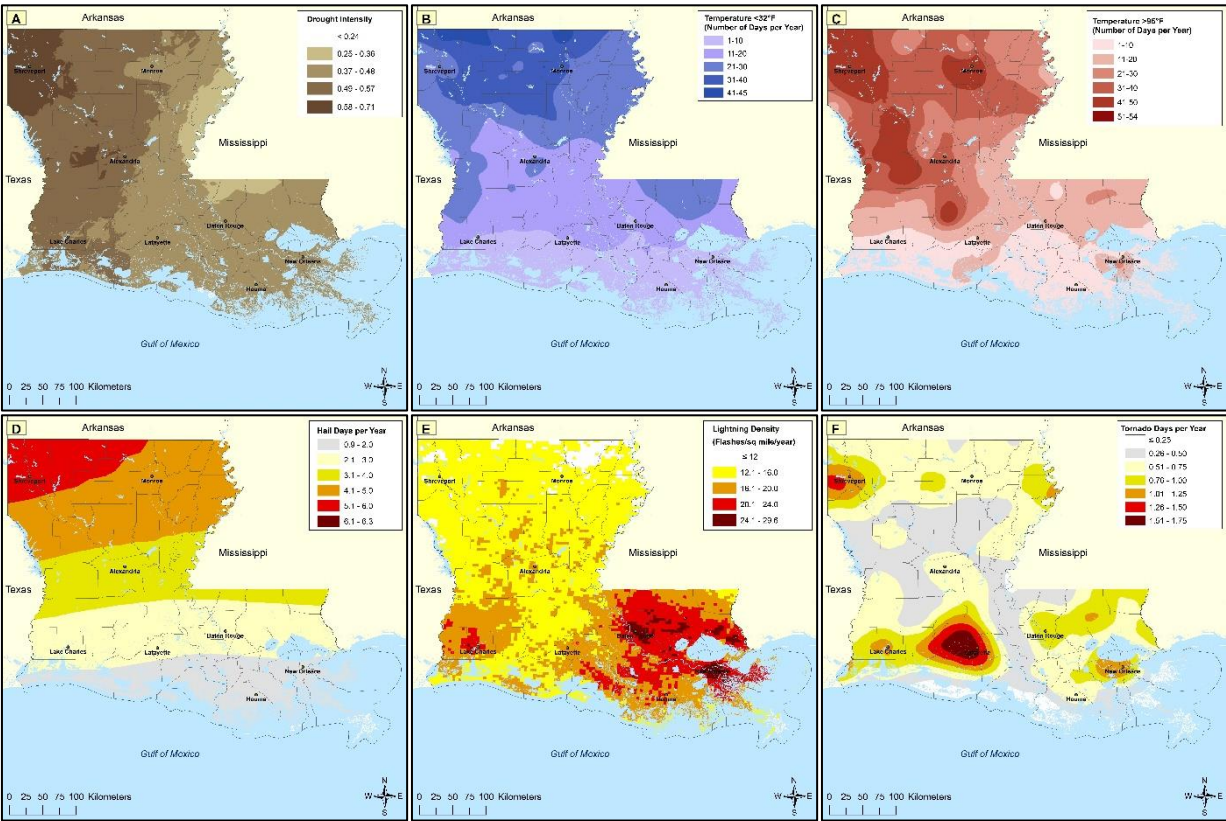


Figure 23. As in Figure 12, but for projected future hazard intensity in Louisiana by 2050.

9.26.2 Historical and Future Projected Change in Crop Land Cover

The majority of crop cultivation occurs in south-central and northeastern Louisiana and along the major river basins (Figure 3A4A). Figure 3B-4B shows the change in crop land cover at the census tract level from 2016 to 2050 in Louisiana. Crop land cover is decreasing in the vast majority of the state, but especially in coastal, north-central, northwestern, and southeastern Louisiana (Figure 3B4B). Increases in crop land cover are sporadic but are mostly in the northeastern part of the state. By 2050, 320 census tracts are projected to have no crop land cover, compared to 207 census tracts in 2016. CLC is projected to increase in only 24 census tracts and decrease in 722 census tracts, with no change projected in 402 census tracts. Urban infringement and abandonment of coastal lands are major reasons for the anticipated decreases.

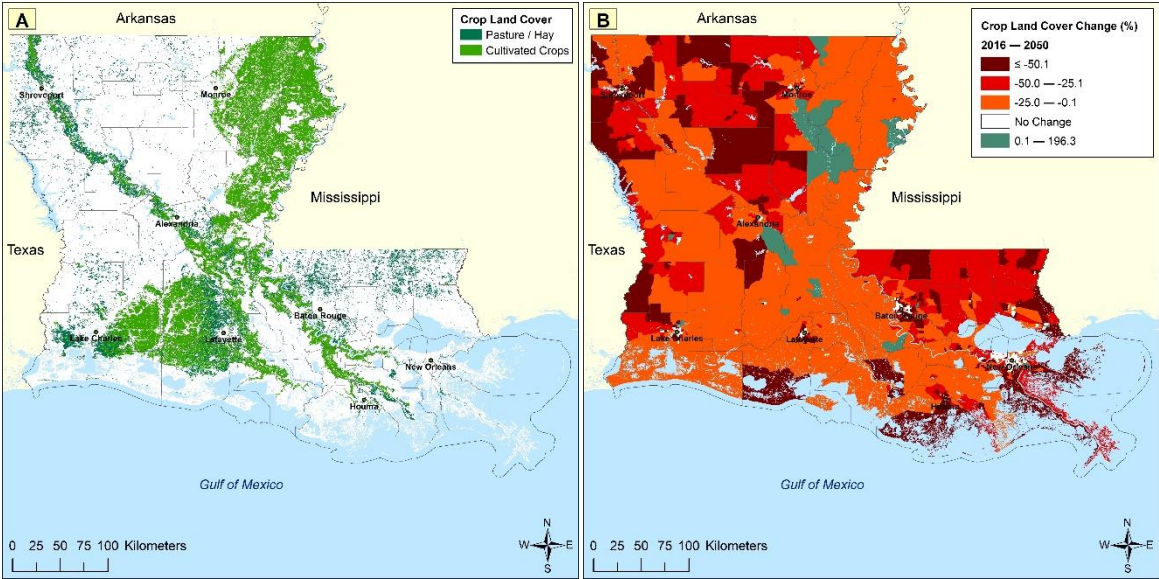


Figure 34. Crop land cover in 2016 (A) and change in crop land cover at the census tract level from 2016 to projection for 2050 (B), in Louisiana.

9.36.3 Historical and Future Projected Annual Crop Loss

Historical annual crop losses due to each of the six hazards in Louisiana are shown in Appendix A. On a statewide basis, drought caused 93.1 percent of historical average annual crop losses from the hazards analyzed here (Table 9). This result is largely consistent with that from Fahad et al. (2017). The relatively smaller positive impact of climate change via extreme cold rather than via extreme heat tends to support the Lesk et al. (2016) position over that of Gu et al. (2008). Caddo (northwestern Louisiana) had the greatest historical annual crop loss due to drought among the parishes (\$6,397,949 or 16.3 percent of Louisiana’s total; Appendix A). Likewise, Terrebonne and Lafourche (south-central Louisiana) and St. James (southeastern Louisiana) experienced the largest historical annual crop loss from extreme

Table 9. Comparison of Louisiana statewide crop loss, by hazard: Historical vs. 2050-projected.

Hazard	Average Annual Crop Loss 1960–2019 (2019\$)	Projected Annual Crop Loss in 2050 (2019\$)	Projected Change (%)
Drought	\$39,196,210	\$56,141,812	43.23%
Extreme Cold	\$1,711,019	\$1,445,347	–15.53%

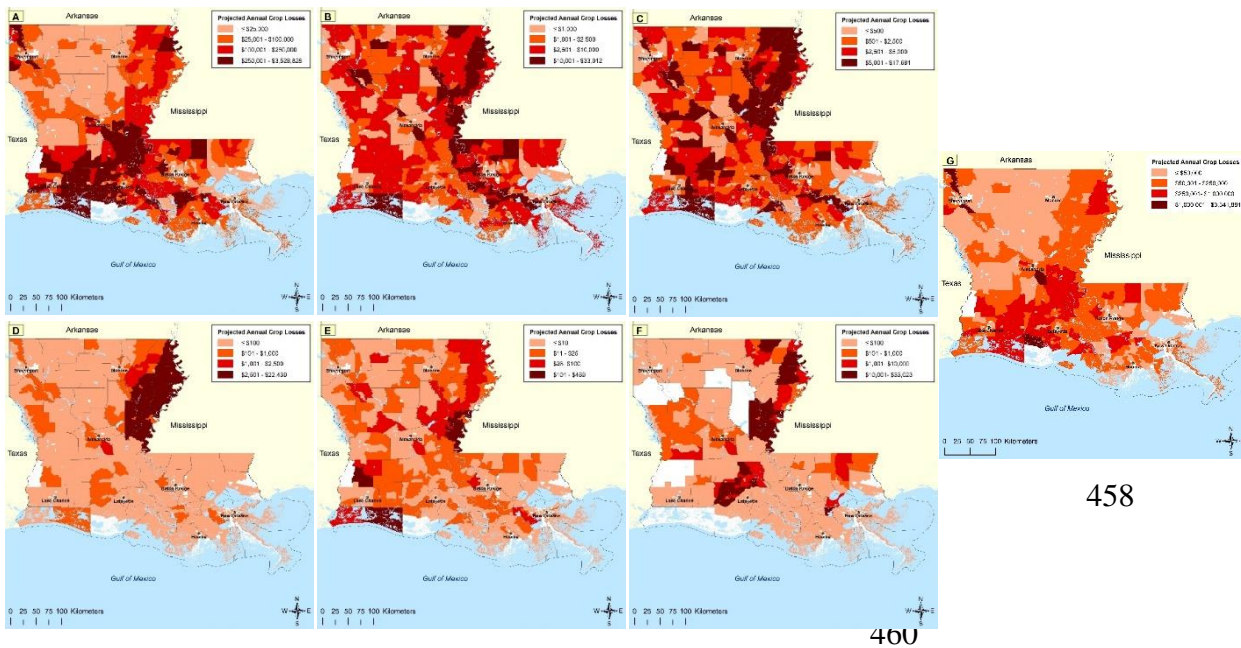
## Louisiana's Future Crop Risk Estimation

Extreme Heat	\$734,551	\$962,216	30.99%
Hail	\$155,956	\$184,450	18.27%
Lightning	\$3,750	\$4,587	22.32%
Tornado	\$316,764	\$444,435	40.30%
Total	\$42,118,250	\$59,182,847	40.52%

436 cold (\$43,647 or 2.6 percent of the statewide total; Appendix A) and hot temperatures (\$14,020 or  
 437 1.9 percent of Louisiana's total; Appendix A), respectively. One caveat of this result is that since  
 438 crop types are not distinguished, it is likely that losses due to high-value crops, such as the citrus  
 439 orchards in Plaquemines Parish, are underestimated in this analysis. Franklin Parish (northeastern  
 440 Louisiana) and Cameron Parish (southwestern Louisiana) had the greatest historical annual crop loss  
 441 due to hail (\$31,070 or 19.9 percent of the statewide total; Appendix A) and lightning (\$439 or 11.7  
 442 percent of Louisiana's total; Appendix A), respectively. Finally, St. Landry Parish in south-central  
 443 Louisiana sustained the highest historical annual crop loss due to tornado (\$77,107 or 24.3 percent of  
 444 the total; Appendix A). No historical crop losses due to tornado were reported for Beauregard,  
 445 Caldwell, Cameron, De Soto, Jackson, La Salle, and Red River parishes.

446 By 2050, total annual crop loss ( $L_{j,2050}$ ), and therefore risk, is expected to increase by about 40.5  
 447 percent (2019\$), with drought comprising 94.9 percent of the total (Table 9). Crop losses due to  
 448 extreme heat, hail, lightning, and tornado are projected to increase substantially but remain relatively  
 449 minor shares of total losses. Of these, hail is an interesting case, because  $L_{j,2050}$  increases despite a  
 450 decreasing future hazard intensity ( $F_{j,2050}$ ) and increasing  $CD_{2050}$ . Extreme cold temperature will  
 451 decrease in  $L_{j,2050}$  due to global warming despite the increased  $CD_{2050}$ .

452 Figure 4A5A-F shows the widely varying ranges for  $L_{j,2050}$  by hazard, as was noted previously in  
 453 Table 9. The absence of crop loss (i.e., risk) in a given area likely infers the absence of crop  
 454 cultivation (e.g., urban census tracts) and/or historical crop loss for that hazard rather than absence of  
 455 severe weather threat.



458

460

461 Figure 45. Projected annual crop loss (2019\$) by Louisiana census tract, 2050: Drought (A), extreme  
462 cold temperature (B), extreme heat (C), hail (D), lightning (E), tornado (F), and total (G).

463 The risk due to drought by 2050 (Figure 4A5A) is projected to be greatest where the combination of  
464 hazard exposure (i.e., northwestern location), cropland (i.e., south-central and northeastern  
465 Louisiana), and a history of crop losses occur (i.e., Caddo, Vermilion, Avoyelles, St. Landry,  
466 Assumption, Calcasieu, and Jefferson Davis parishes). As was the case for historical data, Caddo is  
467 projected to remain the parish with the greatest annual crop loss among the parishes (\$8,386,852 or  
468 14.9 percent of Louisiana's total; Appendix B) by 2050.

469 Projected risk from extreme cold temperature annual crop loss in 2050 (Figure 4B5B) varies  
470 substantially by parish but the risk is relatively evenly distributed throughout Louisiana. Assumption  
471 Parish (south-central Louisiana) may have the highest annual crop loss (\$45,734 or 3.2 percent of the  
472 statewide total) due to extreme cold temperatures in 2050 (Appendix B). The greatest annual  
473 extreme cold temperature loss is projected to be in census tract 22121020300 in West Baton Rouge  
474 Parish of central Louisiana (\$33,011). Extreme heat risk is also projected to be evenly distributed but  
475 is more concentrated in the northeastern part of Louisiana (Figure 4C5C). St. James Parish is  
476 projected to have the highest annual crop loss (\$21,273) among the parishes (2.2 percent of the  
477 state's total; Appendix B). Annual crop loss peaks at \$ 17,681 in census tract 22021000100 within  
478 Caldwell Parish.

479 Interestingly, cold temperatures pose more of a risk than hot temperatures in Louisiana, despite the  
480 projected increased temperatures. It should be noted that extreme heat and the much larger drought  
481 risk go hand-in-hand, so some of the extreme heat risk is likely to be accounted for by the drought  
482 analysis. Also, because cold and heat waves typically engulf large areas, the SHELDUS data resolve  
483 many of the historical crop losses due to extreme cold and heat at a coarse regional scale, causing the  
484 historical annual crop loss values due to extreme heat (and separately, due to extreme cold) to be  
485 assigned equally across many parishes (Appendix A). The method employed here allows projected  
486 loss to vary across parishes by distributing the loss based on current and projected changes to land  
487 cover by census tract and spatial variability in hazard intensity (Appendix B).



488 The crop risk to the hail hazard in 2050 is projected to peak in northeastern Louisiana, including  
489 Catahoula, Concordia, East Carroll, Franklin, Madison, and Tensas parishes (Figure ~~4D~~5D).  
490 Franklin Parish is projected to have the greatest annual crop loss among the parishes (\$38,442 or 20.8  
491 percent of Louisiana's total; Appendix B). The census tract with the highest projected annual crop  
492 loss due to hail (\$22,439 in census tract 22065960200) is in Madison Parish.

493 Lightning risk is projected to peak in sparsely-populated southwestern and northeastern Louisiana  
494 (Figure ~~4E~~5E) where hazard, CLC, and historical crop loss overlap. This spatial peak in risk occurs  
495 despite a higher hazard intensity elsewhere (see again Figure ~~2E~~3E), as the higher hazard intensity is  
496 occurring in largely non-agricultural areas. Cameron Parish is projected to have the greatest annual  
497 crop loss (\$561) among the parishes (12.2 percent of Louisiana's total; Appendix B). Annual crop  
498 loss peaks at \$468 in Cameron Parish (census tract 22023970100), likely because it is one of the few  
499 tracts in Cameron with intense cultivation.

500 Tornado risk is anticipated to remain much higher than that of hail and lightning. Acadia Parish in  
501 southwestern Louisiana is projected to have the highest annual crop loss (\$112,376 or 25.3 percent of  
502 the state total) due to tornado in 2050 (Appendix B). At the census tract scale, peak losses are  
503 projected to be in the large, northeastern Louisiana census tracts in Catahoula, Concordia,  
504 Morehouse, southern East Carroll, and western Madison parishes (Figure ~~4F~~5F). The greatest annual  
505 tornado loss is in census tract 22095071100 in St. John the Baptist Parish (\$33,022).

#### 9.56.4 Sensitivity Analysis

A brief sensitivity analysis to demonstrate the impact of different model assumptions regarding future conditions for each hazard, taken one at a time, is presented in Table 10. The final column in Table 10 shows the estimated change in annual crop loss if an underestimate or overestimate in modeled values of ten percentage points occurs. Interestingly, due to compensating effects of hazard intensities that are projected to increase (i.e., drought, extreme heat, lightning, and tornado) vs. those expected to decrease (i.e., extreme cold and hail), an “across-the-board” underestimation or overestimation for all six hazards leads to bulk total property losses that change by only  $\pm 7.5$  percent (i.e., bottom row of Table 10).

**Table 10** Sensitivity analysis of annual crop loss (i.e., risk) estimates statewide in Louisiana for each hazard by 2050, for 10 percent overestimation or underestimation of the hazard intensity change (2019\$).

Hazard	Overestimate $F_{j,x}$ by 10 percent	Modeled $F_{j,x}$ (Equation 6)	Underestimate $F_{j,x}$ by 10 percent	Difference from Equation 6
Drought	\$60,633,159 (+35%)	\$56,141,812 (+25%)	\$51,650,468 (+15%)	$\pm 8.0\%$
Extreme Cold	\$1,264,683 (−30%)	\$1,445,347 (−20%)	\$1,626,021 (−10%)	$\pm 12.5\%$
Extreme Heat	\$1,042,399 (+30%)	\$962,216 (+20%)	\$882,030 (+10%)	$\pm 8.3\%$
Hail	\$163,953 (−20%)	\$184,450 (−10%)	\$204,941 (0%)	$\pm 11.1\%$
Lightning	\$5,006 (+20%)	\$4,587 (+10%)	\$4,172 (0%)	$\pm 9.1\%$
Tornado	\$484,836 (+20%)	\$444,435 (+10%)	\$404,030 (0%)	$\pm 9.1\%$
Total	\$63,594,036	\$59,182,847	\$54,771,662	$\pm 7.5\%$

#### 107 Study Limitations

Because of the lack of model-output data with high confidence at the sub-state scale, the geographical distribution of the hazards is assumed to be constant over space throughout Louisiana. Similarly, projected temporal changes in hazard intensity by 2050 are assumed to be consistent statewide. In reality, changing frequencies and intensities of synoptic weather patterns that produce extreme weather conditions will not be consistent across space, even at the sub-state scale.

The reliability of the crop loss as projected for the year 2050 depends on the accuracy of input data (i.e., historical hazard intensity, historic crop loss, and crop market and export values) and model estimations (i.e., future hazard conditions, future crop land cover changes, population projection, changing consumer demand, cropping intensity, and technological development). The consideration of annual values can introduce inaccuracies and uncertainties, as climate changes are assumed to occur differently by season, yet the climate model uncertainties still lag behind uncertainties of other models, such as hydrological, at the seasonal scale (Joseph et al. 2018). Human cultural and economic changes, including wealth/GDP, product preferences, adaptations (e.g., changing competition from other producers), and policy are not incorporated in the study.

This study's source for historic crop losses (SHELDUS) has limitations. First, despite including loss estimates across all hazard types and magnitudes, gaps and biases in these estimates exist in SHELDUS. For example, because SHELDUS assumed the lower bound of the logarithmic range (e.g., \$5,000 to \$50,000) that NOAA's NCEI (NCDC at the time) had been using to report loss estimates prior to 1996, losses tended to be underestimated for the earlier decades. Furthermore, indirect losses, including employment hours, health problems during evacuation, and complications caused by other storm-induced stressors, are not included (Gall et al. 2009). A known issue with loss databases and their application to projections of losses is how compound events are categorized. Zscheischler et al. (2018) acknowledged that loss underestimates could occur due to the accounting of compound events as only one hazard type. In the case of the present analysis, given that SHELDUS losses are divided equally, some errors are naturally introduced and unavoidable as the U.S. National Weather Service, the data source for SHELDUS, reports losses as compound event totals only and forgoes estimation by hazard type. A final limitation regarding the crop loss data is that because SHELDUS did not itemize crop loss by crop, the data availability necessitated a "bulk" analysis of all crops, which in fact masks the influences of different climatic extremes on the individual crops.

Data management decisions by the responsible agencies can also introduce uncertainties when used for purposes in this research. For example, although the U.S. National Weather Service strives to collect county-scale loss data, losses from some events are reported only at the multi-county scale. In such cases, SHELDUS partitions losses equally among the affected counties, regardless of differences in population, population density, or development. Because the scale of such events is so broad, the most glaring example of this type of generalization of losses is for extreme heat; nearly all parishes were assigned the same historical crop loss value (Appendix A). Despite the limitations, SHELDUS data have been used successfully in similar research (e.g., Li et al. 2015; Rohli et al. 2016; Hahn et al. 2017; Paul and Sharif 2018; Mostafiz et al. 2020b) and remains the best available source for U.S. hazard-induced crop loss data.

## **118 Summary and Conclusions**

This study offers an approach for improving risk estimates for six important weather hazards using the example of Louisiana, one of the most weather-vulnerable U.S. states. The method avoids, where possible, aggregating data to a county-level risk. The finer-resolution spatial analysis is valuable because uneven population distribution and/or hazard exposure often makes the scale of natural hazard-induced damage, and therefore the risk, spatially heterogeneous and/or localized. This work also circumvents another perennial complication in risk assessment by incorporating estimates of future changes in both the local hazard intensity and crop land cover; one or both of these factors are often ignored in projecting risk. While our approach certainly cannot avoid making gross

assumptions, the use of localized, weighted, model-based projections of crop land cover, consumer demand, and future hazard intensities to estimate census-tract-level risk of crop loss due to several severe weather hazards in Louisiana, U.S.A., by 2050, enhances our current understanding of current and future severe weather impacts.

The major findings of this research are:

- While the majority of cropland occurs and will continue to occur in south-central and northeastern Louisiana along the river basins, crop activity is decreasing in southeastern and northwestern Louisiana and is increasing in parts of the northeast.
- By 2050, crop risk, measured as likelihood of economic loss, statewide is likely to continue to be dominated by drought, which is projected to account for \$56 million of the \$59 million (~95%) in crop loss by 2050.
- Extreme cold is likely to continue to produce more damage than extreme heat (although the latter often occurs in tandem with drought), despite the projected warming climate.
- Tornadoes, hail, and lightning will remain the fourth, fifth, and sixth riskiest hazards examined, respectively.
- The northeastern part of the state can be expected to remain impacted relatively more heavily than other parts of the state by extreme heat, hail, lightning, and tornadoes.

The findings in this study will help decision-makers to make crops more resilient to future hazards, thereby strengthening the economically-important agriculture industry in Louisiana and enhancing food security.

Work based on a similar methodology is needed to evaluate future risk from other hazards in other locations. Moreover, more sophisticated projections of cropland, consumer demand, cropping intensity, technological development, and demography will improve model projections of future losses, enhancing decision-making for allocating resources to mitigate and adapt to these natural hazards.



596 **129** **Supplementary Material**

597 Appendix A: Historical Annual Crop Loss (2019\$), by Louisiana Parish

Parish	Crop Loss (2019\$)					
	Drought	Extreme Cold	Extreme Heat	Hail	Lightning	Tornado
Acadia	1,371,710	16,079	11,437	808	40	76,987
Allen	788,538	16,079	11,437	123	40	170
Ascension	242,710	42,657	11,437	123	40	11
Assumption	1,594,103	42,657	11,437	479	40	60
Avoyelles	2,519,244	18,443	11,437	123	70	152
Beauregard	735,927	16,079	11,437	330	296	-
Bienville	58,452	19,786	11,437	132	41	11
Bossier	127,274	19,786	11,437	123	41	104
Caddo	6,397,949	19,786	11,437	1,589	41	154
Calcasieu	1,490,853	16,079	11,437	123	40	4
Caldwell	58,452	19,786	11,437	160	43	-
Cameron	242,587	16,079	11,437	123	439	-
Catahoula	133,636	18,443	11,437	16,457	40	21,006
Claiborne	58,452	19,786	11,437	123	41	208
Concordia	146,806	18,443	11,437	14,543	372	23,519
De Soto	127,274	19,786	11,437	514	41	-
East Baton Rouge	415,216	42,657	11,437	420	40	11
East Carroll	222,716	19,786	11,437	15,453	78	15,635
East Feliciana	684,855	42,657	11,437	126	40	269
Evangeline	882,598	17,701	11,437	596	40	11
Franklin	174,632	19,786	11,437	31,070	41	5
Grant	58,452	18,443	11,437	140	40	95
Iberia	714,983	16,079	11,437	123	40	11
Iberville	333,698	42,657	11,437	123	40	11
Jackson	58,452	19,786	11,437	160	41	-
Jefferson	233,367	42,657	11,437	260	40	27

# Louisiana's Future Crop Risk Estimation

Jefferson Davis	1,484,583	16,079	11,437	123	40	16
La Salle	58,452	16,079	11,437	299	40	20
Lafayette	1,365,440	43,647	11,437	131	40	11
Lafourche	396,404	18,443	11,437	123	40	-
Lincoln	58,452	19,786	11,437	181	41	70
Livingston	684,855	42,657	11,437	123	40	536
Madison	182,213	20,170	11,437	25,835	41	19,869
Morehouse	199,812	19,786	11,437	543	41	17,670
Natchitoches	58,452	18,443	11,437	176	40	1,482
Orleans	233,367	42,657	11,437	260	40	11
Ouachita	58,452	19,786	11,437	892	41	27
Plaquemines	233,367	43,590	11,437	326	40	11
Pointe Coupee	622,149	41,105	11,437	123	40	11
Rapides	1,252,568	18,443	11,437	2,027	40	4,301
Red River	58,452	19,786	11,437	131	41	-
Richland	198,486	20,170	11,437	4,504	41	23
Sabine	127,274	18,443	11,437	2,180	40	1,789
St. Bernard	233,367	42,599	11,437	260	40	11
St. Charles	252,179	42,657	11,437	260	40	11
St. Helena	1,042,284	42,657	11,437	123	40	269
St. James	571,983	42,657	14,020	123	40	11
St. John the Baptist	233,367	42,657	11,437	123	40	33,875
St. Landry	2,387,560	16,079	11,437	525	70	77,107
St. Martin	794,808	16,079	11,437	123	40	11
St. Mary	850,843	16,079	11,437	123	40	11
St. Tammany	233,367	42,999	11,437	123	40	11
Tangipahoa	233,367	42,999	11,437	123	40	10,094
Tensas	155,808	19,786	11,437	27,388	41	2,212
Terrebonne	352,510	43,647	11,437	158	40	11
Union	58,452	19,786	11,437	396	60	2

## Louisiana's Future Crop Risk Estimation

Vermilion	2,951,921	16,079	11,437	131	40	20
Vernon	4,928	18,443	11,437	165	40	4,484
Washington	747,562	42,657	11,437	123	45	3,694
Webster	58,452	19,786	11,437	146	41	2
West Baton Rouge	277,261	42,657	11,437	123	40	11
West Carroll	199,516	19,786	11,437	2,652	98	242
West Feliciana	352,510	41,105	11,437	123	40	11
Winn	58,452	18,786	11,437	336	41	356
Total Loss	39,196,210	1,711,019	734,551	155,956	3,750	316,764

598

599 Source: CEMHS, 2020.

600 Appendix B: Projected Annual Crop Loss in 2050 (2019\$), by Louisiana Parish

Parish	Projected Annual Crop Loss in 2050 (2019\$)					
	Drought	Extreme Cold	Extreme Heat	Hail	Lightning	Tornado
Acadia	2,275,459	17,071	18,209	965	59	112,376
Allen	1,137,445	14,674	15,588	127	51	217
Ascension	321,556	35,377	14,002	116	46	13
Assumption	2,671,920	45,734	18,394	578	59	88
Avoyelles	4,132,621	19,349	18,044	145	100	220
Beauregard	828,671	11,594	12,305	268	293	-
Bienville	66,541	14,388	12,595	108	41	11
Bossier	156,079	15,625	13,476	108	44	111
Caddo	8,386,852	16,811	14,342	1,504	47	171
Calcasieu	2,204,443	14,811	15,909	130	52	5
Caldwell	99,850	21,572	18,794	197	64	-
Cameron	351,941	14,919	15,920	128	561	-
Catahoula	224,030	19,845	18,444	19,880	59	30,998
Claiborne	68,355	14,670	12,907	102	42	219
Concordia	243,984	19,562	18,248	17,385	543	34,285
De Soto	98,738	9,933	8,791	288	28	-
East Baton Rouge	510,054	33,670	13,501	372	43	12
East Carroll	375,350	21,342	18,504	18,751	116	23,187
East Feliciana	631,269	24,536	10,350	83	33	227
Evangeline	1,404,425	17,911	17,569	681	56	16
Franklin	300,517	21,792	18,880	38,442	62	7
Grant	83,786	16,587	15,577	144	50	121
Iberia	1,141,124	16,446	17,515	141	56	16
Iberville	536,375	43,963	17,600	142	56	16
Jackson	51,487	11,069	9,569	101	32	-
Jefferson	257,026	29,614	12,433	206	39	26
Jefferson Davis	2,444,470	16,954	18,130	145	58	24

# Louisiana's Future Crop Risk Estimation

La Salle	54,334	10,914	10,162	200	33	-
Lafayette	1,947,984	14,744	15,709	135	50	25
Lafourche	588,372	41,671	16,725	132	52	15
Lincoln	61,308	13,370	11,614	137	38	65
Livingston	734,050	28,832	11,683	93	38	500
Madison	299,845	21,221	18,081	30,595	59	28,717
Morehouse	324,259	20,407	17,759	635	59	25,194
Natchitoches	85,289	17,164	16,006	185	51	1,899
Orleans	361,063	42,038	17,260	288	55	15
Ouachita	87,164	18,721	16,340	955	54	35
Plaquemines	88,440	10,846	4,681	99	13	5
Pointe Coupee	1,032,358	43,654	18,211	146	59	16
Rapides	2,017,682	19,209	17,767	2,359	57	6,243
Red River	76,935	16,672	14,454	124	48	-
Richland	333,421	21,686	18,460	5,445	61	34
Sabine	169,667	15,690	14,677	2,089	47	2,107
St. Bernard	278,537	30,879	12,757	215	41	12
St. Charles	367,728	39,767	16,132	271	51	14
St. Helena	926,352	24,271	9,759	78	31	211
St. James	908,940	43,297	21,273	140	56	16
St. John the Baptist	339,259	39,316	15,891	128	51	43,678
St. Landry	3,917,850	16,885	18,018	621	100	111,209
St. Martin	1,288,165	16,706	17,879	143	57	16
St. Mary	1,374,866	16,769	17,830	143	57	16
St. Tammany	233,190	28,140	11,260	89	35	10
Tangipahoa	242,131	28,324	11,275	91	37	9,188
Tensas	261,997	21,302	18,458	33,163	61	3,275
Terrebonne	392,863	29,947	13,108	127	39	12
Union	68,873	14,977	12,930	336	62	2
Vermilion	4,180,319	14,796	15,474	135	50	27
Vernon	7,074	16,849	15,780	170	51	5,641

Washington	765,472	28,048	11,277	90	41	3,335
Webster	66,731	14,373	12,567	120	41	2
West Baton Rouge	452,465	44,606	17,979	144	58	16
West Carroll	330,545	20,971	18,185	3,162	143	353
West Feliciana	443,004	32,579	13,771	111	43	11
Winn	28,912	5,887	5,428	119	18	155
Total Loss	56,141,812	1,445,347	962,216	184,450	4,587	444,435

601  
602  
603  
604



606  
607  
608  
609  
610  
611  
612  
613  
614  
615  
616  
617  
618  
619  
620  
621  
622  
623  
624  
625  
626

**1310 Conflict of Interest**

*The authors declare that the research was conducted in the absence of any commercial or financial relationships that could be construed as a potential conflict of interest.*

**1411 Author Contributions**

RBM developed the detailed methodology, collected and analyzed the data, and developed the initial text. RR developed the atmospheric projections and edited early and late drafts of the text. CF conceptualized the hazard quantification and census tract methodologies and revised the text. MG provided the SHELDUS data and revised the text. NB provided oversight on analysis, particularly regarding the crop land cover projections, and revised the text.

**1512 Funding**

This project resulted from the 2019 Louisiana State Hazard Mitigation Plan update, for which CF and RR received funding from FEMA, via GOHSEP, grant number: 2000301135. Any opinions, findings, conclusions, and recommendations expressed in this manuscript are those of the authors and do not necessarily reflect the views of FEMA or GOHSEP.

**1613 Acknowledgments**

The authors warmly appreciate the assistance of Jeffrey Giering of Louisiana's Governor's Office of Homeland Security and Emergency Preparedness (GOHSEP) for overall project support, David Dunaway of LSU Libraries for assistance in acquiring agricultural data, and Dr. Thanos Gentimis of LSU for statistical guidance.



## 1714 References

- Annan, F., & Schlenker, W. (2015). Federal crop insurance and the disincentive to adapt to extreme heat. *American Economic Review*, 105(5), 262–266. doi:10.1257/aer.p20151031
- Brooks, H. E. (2013). Severe thunderstorms and climate change. *Atmospheric Research*, 123(2013), 129–138. doi:10.1016/j.atmosres.2012.04.002
- Brooks, W., Barnett, D. H., Harrison, W. A., Hattz, D., Mankowski, J., Dickens, J., & Neuber, A. (2020). Investigation of lightning attachment risks to small structures associated with the electrogeometric model (EGM). *IEEE Transactions on Plasma Science*, 48(6), 2163–2174. doi:10.1109/TPS.2020.2989664
- Bushra, N., Mostafiz, R. B., Rohli, R. V., Friedland, C. J., and Rahim, M. A. (2021). Technical and social approaches to study shoreline change of Kualkata, Bangladesh. *Frontiers in Marine Science*, 8, Art. No. 730984. doi: 10.3389/fmars.2021.730984.
- Bushra, N., Rohli, R. V., Lam, N. S., Zou, L., Mostafiz, R. B., and Mihunov, V. (2019). The relationship between the normalized difference vegetation index and drought indices in the South Central United States. *Natural Hazards*, 96(2), 791-808. doi: 10.1007/s11069-019-03569-5.
- Center for Emergency Management and Homeland Security (CEMHS). (2020). Spatial Hazard Events and Losses Database for the United States, Version 19.0. Center for Emergency Management and Homeland Security, Arizona State University. <https://cemhs.asu.edu/sheldus> [Accessed February 11, 2021].
- Changnon, S. A. (1972). Examples of economic losses from hail in the United States. *Journal of Applied Meteorology and Climatology*, 11(7), 1128–1137.
- Changnon, S. A., Changnon, J. M., & Hewings, G. J. (2001). Losses caused by weather and climate extremes: A national index for the United States. *Physical Geography*, 22(1), 1–27. doi:10.1080/02723646.2001.10642727
- Cutter, S., Osman-Elasha, B., Campbell, J., Cheong, S. M.-, McCormick, S., Pulwarty, R., Supratid, S., & Ziervogel, G. (2012). Managing the risks from climate extremes at the local level. In: *Managing the Risks of Extreme Events and Disasters to Advance Climate Change Adaptation* [Field, C.B., Barros, V., Stocker, T. F., Qin, D., Dokken, D. J., Ebi, K. L., Mastrandrea, M. D., Mach, K. J., Plattner, G.- K., Allen, S. K., Tignor, M., & Midgley, P. M. (eds.)]. A Special Report of Working Groups I and II of the Intergovernmental Panel on Climate Change (IPCC). Cambridge University Press, Cambridge, UK, and New York, NY, USA, 291–338.
- Easterling, D. R., Kunkel, K. E., Arnold, J. R., Knutson, T., LeGrande, A. N., Leung, L. R., Vose, R. S., Waliser, D. E., & Wehner, M. F. (2017). Precipitation change in the United States. In: *Climate Science Special Report: Fourth National Climate Assessment, Volume I* [Wuebbles, D. J., Fahey, D. W., Hibbard, K. A., Dokken, D. J., Stewart, B. C., & Maycock, T. K. (eds.)]. U.S. Global Change Research Program, Washington, DC, USA, pp. 207–230. doi:10.7930/J0H993CC
- Eck, M. A., Murray, A. R., Ward, A. R., & Konrad, C. E. (2020). Influence of growing season temperature and precipitation anomalies on crop yield in the southeastern United States. *Agricultural and Forest Meteorology*, 291(2020), Art. No. 108053. doi:10.1016/j.agrformet.2020.108053

- Epanechnikov, V. A. (1969). Nonparametric estimation of a multidimensional probability density. *Theory of Probability and Its Applications*, 14(1), 153–158.
- [Fahad, S., Bajwa, A. A., Nazir, U., Anjum, S. A., Farooq, A., Zohaib, A., Sadia, S., Nasim, W., Adkins, S., Saud, S., Ihsan, M. Z., Alharby, H., Wu, C., Wang, D. P., Huang, J. L. \(2017\). Crop production under drought and heat stress: Plant responses and management Options. \*Frontiers in Plant Science\*, 8, Art. No. 1147. doi:10.3389/fpls.2017.01147](#)
- Foley, J. A., Ramankutty, N., Brauman, K. A., Cassidy, E. S., Gerber, J. S., Johnston, M., Mueller, N. D., O'Connell, C., Ray, D. K., West, P. C., & Balzer, C. (2011). Solutions for a cultivated planet. *Nature*, 478(7369), 337–342. doi:10.1038/nature10452
- Forzieri, G., Cescatti, A., e Silva, F. B., & Feyen, L. (2017). Increasing risk over time of weather-related hazards to the European population: A data-driven prognostic study. *The Lancet Planetary Health*, 1(5), e200–e208. doi:10.1016/S2542-5196(17)30082-7
- Franzke, C. L., & Czuptyna, M. (2020). Probabilistic assessment and projections of US weather and climate risks and economic damages. *Climatic Change*, 158(3), 503–515. doi:10.1007/s10584-019-02558-8
- Gall M., Borden, K. A., & Cutter, S. L. (2009). When do losses count? Six fallacies of natural hazards loss data. *Bulletin of the American Meteorological Society*, 90(6), 799–809. doi:10.1175/2008BAMS2721.1
- Gensini, V.A., Ramseyer, C., & Mote, T. L. (2014). Future convective environments using NARCCAP. *International Journal of Climatology*, 34(5), 1699–1705. doi:10.1002/joc.3769.
- [Gnan, E., Friedland, C. J., Rahim, M. A., Mostafiz, R. B., Rohli, R. V., Orooji, F., Taghinezhad, A., & McElwee, J. \(2022a\). Improved building-specific flood risk assessment and implications for depth-damage function selection. In review at Frontiers in Water, section Water and Hydrocomplexity since 5/10/2022.](#)
- [Gowda, P., Steiner, J. L., Olson, C., Boggess, M., Farrigan, T., & Grusak, M. A. \(2018\). Agriculture and rural communities. In \*Impacts, Risks, and Adaptation in the United States: Fourth National Climate Assessment, Volume II\* \[Reidmiller, D. R., Avery, C. W., Easterling, D. R., Kunkel, K. E., Lewis, K. L. M., Maycock, T. K., & Stewart, B. C. \(eds.\)\]. U.S. Global Change Research Program, Washington, DC, USA, 391–437. doi:10.7930/NCA4.2018.CH10](#)
- [Gnan, E., Friedland, C. J., Mostafiz, R. B., Rahim, M. A., Gentimis, T., Taghinezhad, A., & Rohli, R. V. \(2022b\). Economically optimizing elevation of new, single-family residences for flood mitigation via life-cycle benefit-cost analysis. \*Frontiers in Environmental Science\*, 10:889239. doi: 10.3389/fenvs.2022.889239.](#)
- [Gowda, P., Steiner, J. L., Olson, C., Boggess, M., Farrigan, T., & Grusak, M. A. \(2018\). Agriculture and rural communities. In \*Impacts, Risks, and Adaptation in the United States: Fourth National Climate Assessment, Volume II\* \[Reidmiller, D. R., Avery, C. W., Easterling, D. R., Kunkel, K. E., Lewis, K. L. M., Maycock, T. K., & Stewart, B. C. \(eds.\)\]. U.S. Global Change Research Program, Washington, DC, USA, 391–437. doi:10.7930/NCA4.2018.CH10](#)
- [Gu, L., Hanson, P. J., Mac Post, W., Kaiser, D. P., Yang, B., Nemani, R., Pallardy, S. G., & Meyers, T. \(2008\). The 2007 eastern US spring freezes: Increased cold damage in a warming world? \*Bioscience\*, 58\(3\), 253–262. doi:10.1641/B580311](#)

- 712 Guo, E., Liu, X., Zhang, J., Wang, Y., Wang, C., Wang, R., & Li, D. (2017). Assessing  
713 spatiotemporal variation of drought and its impact on maize yield in Northeast China. *Journal*  
714 *of Hydrology*, 553(2017), 231–247. doi:10.1016/j.jhydrol.2017.07.060
- 715 Hahn, D. J., Emmanuelle, E., & Corotis, R. B. (2017). Multihazard mapping of the United States.  
716 *Journal of Risk and Uncertainty in Engineering Systems, Part A: Civil Engineering*, 3(3), Art.  
717 No. 04016016. doi:10.1061/AJRUA6.0000897
- 718 He, Y., Lindbergh, S., Graves, C., & Rakas, J. (2020). Airport exposure to lightning strike hazard in  
719 the contiguous United States. *Risk Analysis*, in press. doi:10.1111/risa.13630.
- 720 Hinkel, J., Nicholls, R. J., Vafeidis, A. T., Tol, R. S., & Avagianou, T. (2010). Assessing risk of and  
721 adaptation to sea-level rise in the European Union: an application of DIVA. *Mitigation and*  
722 *Adaptation Strategies for Global Change*, 15(7), 703–719. doi:10.1007/s11027-010-9237-y
- 723 Hosseini, M., Kerner, H. R., Sahajpal, R., Puricelli, E., Lu, Y. H., Lawal, A. F., Humber, M. L.,  
724 Mitkish, M., Meyer, S., & Becker-Reshef, I. (2020). Evaluating the impact of the 2020 Iowa  
725 derecho on corn and soybean fields using synthetic aperture radar. *Remote Sensing*, 12(23),  
726 Art. No. 3878. doi:10.3390/rs12233878
- 727 Jonkman, S. N. (2005). Global perspectives on loss of human life caused by floods. *Natural Hazards*,  
728 34(2), 151–175. doi:10.1007/s11069-004-8891-3
- 729 Joseph, J., Ghoshab, S., Pathaka, A., & Sahaic, A. K. (2018). Hydrologic impacts of climate change:  
730 Comparisons between hydrological parameter uncertainty and climate model uncertainty.  
731 *Journal of Hydrology*, 10.1016/j.jhydrol.2018.08.080
- 732 Kebede, A. S., & Nicholls, R. J. (2012). Exposure and vulnerability to climate extremes: population  
733 and asset exposure to coastal flooding in Dar es Salaam, Tanzania. *Regional Environmental*  
734 *Change*, 12(1), 81–94. doi:10.1007/s10113-011-0239-4
- 735 Kocur-Bera, K. (2018). A safe space of rural areas in the context of the occurrence of extreme  
736 weather events-A case study covering a part of the Euroregion Baltic. *Land Use Policy* 71,  
737 518–529. doi:10.1016/j.landusepol.2017.11.013
- 738 Kogan, F., Goldberg, M., Schott, T., & Guo, W. (2015). Suomi NPP/VIIRS: improving drought  
739 watch, crop loss prediction, and food security. *International Journal of Remote Sensing*,  
740 36(21), 5373–5383. doi:10.1080/01431161.2015.1095370
- 741 Lam, N. S. N., Reams, M., Li, K., Li, C., & Mata L. P. (2016). Measuring community resilience to  
742 coastal hazards along the northern Gulf of Mexico. *Natural Hazards Review*, 17(1), Art. No.  
743 04015013. doi:10.1061/(ASCE)NH.1527-6996.0000193
- 744 Lam, N. S. N., Qiang, Y., Li, K., Cai, H., Zou, L., & Mihunov, V. (2018). Extending resilience  
745 assessment to dynamic system modeling: Perspectives on human dynamics and climate  
746 change research. *Journal of Coastal Research*, 85(10085), 1401–1405. doi:10.2112/SI85-  
747 281.1
- 748 Leigh, R., & Kuhnel, I. (2001). Hailstorm loss modelling and risk assessment in the Sydney region,  
749 Australia. *Natural Hazards*, 24(2), 171–185. doi:10.1023/A:1011855801345
- 750 Leng, G., & Hall, J. (2019). Crop yield sensitivity of global major agricultural countries to droughts  
751 and the projected changes in the future. *Science of the Total Environment*, 654, 811–821.  
752 doi:10.1016/j.scitotenv.2018.10.434
- 753 Lesk, C., Rowhani, P. & Ramankutty, N. (2016). Influence of extreme weather disasters on global  
754 crop production. *Nature*, 529(7584), 84–87. <https://doi.org/10.1038/nature16467>

- Li, K., Lam, N. S., Qiang, Y., Zou, L., & Cai, H. (2015). A cyberinfrastructure for community resilience assessment and visualization. *Cartography and Geographic Information Science*, 42(sup1), 34–39. doi:10.1080/15230406.2015.1060113
- Masoomi, H., & van de Lindt, J. W. (2018). Restoration and functionality assessment of a community subjected to tornado hazard. *Structure and Infrastructure Engineering*, 14(3), 275–291. doi:10.1080/15732479.2017.1354030
- Mills, B. (2020). An updated assessment of lightning-related fatality and injury risk in Canada: 2002–2017. *Natural Hazards: Journal of the International Society for the Prevention and Mitigation of Natural Hazards*, 1–13. doi:10.1007/s11069-020-03942-9
- Mostafiz, R. B., Friedland, C., Rohli, R. V., & Bushra, N. (2020a). Assessing Property Loss in Louisiana, U.S.A., to Natural Hazards Incorporating Future Projected Conditions. In *AGU Fall Meeting Abstracts* (Vol. 2020, pp. NH015-0002). <https://ui.adsabs.harvard.edu/abs/2020AGUFMNH0150002M/abstract> [Accessed November 23, 2021].
- Mostafiz, R. B., Friedland, C., Rohli, R. V., Gall, M., Bushra, N., & Gilliland, J. M. (2020b). Census-block-level property risk estimation due to extreme cold temperature, hail, lightning, and tornadoes in Louisiana, USA. *Frontiers in Earth Science*, 8, Art. No. 601624. doi:10.3389/feart.2020.601624
- Mostafiz, R. B., Bushra, N., Rohli, R. V., Friedland, C. J., & Rahim, M. A. (2021a). Present vs. future property losses from a 100-year coastal flood: A case study of Grand Isle, Louisiana. *Frontiers in Water*, 3, Art. No. 763358. doi: 10.3389/frwa.2021.763358.
- Mostafiz, R. B., Friedland, C. J., Rohli, R. V., & Bushra, N. (2021b). Property risk assessment of sinkhole hazard in Louisiana, U.S.A. *Frontiers in Environmental Science*, 9, Art. No. 780870. doi: 10.3389/fenvs.2021.780870.
- Mostafiz, R. B., Friedland, C. J., Rohli, R. V., Bushra, N., & Held, C. L. (2021c). Property risk assessment for expansive soils in Louisiana. *Frontiers in Built Environment*, 7, Art. No. 754761. doi: 10.3389/fbuil.2021.754761.
- Mostafiz, R. B., Friedland, C. J., Rahman, M. A., Rohli, R. V., Tate, E., Bushra, N., & Taghinezard, A. (2021d). Comparison of neighborhood-scale, residential property flood-loss assessment methodologies. *Frontiers in Environmental Science*, 9, Art. No. 734294. doi: 10.3389/fenvs.2021.734294.
- Mostafiz, R. B., Friedland, C. J., Rohli, R. V., & Bushra, N. (2022a). Estimating Future Residential Property Risk Associated with Wildfires in Louisiana, U.S.A. *Climate*, 10(4). doi: 10.3390/cli10040049.
- Mostafiz, R. B., Rohli, R. V., Friedland, C. J., & Lee, Y. C. (2022b). Actionable Information in Flood Risk Communications and the Potential for New Web-Based Tools for Long-term Planning for Individuals and Community. *Frontiers in Earth Science*, 10, Art. No. 840250. doi: 10.3389/feart.2022.840250
- Mostafiz, R.B. (2022c). " Estimation of Economic Risk from Coastal Natural Hazards in Louisiana". *LSU Doctoral Dissertations*. 5880. [https://digitalcommons.lsu.edu/gradschool\\_dissertations/5880](https://digitalcommons.lsu.edu/gradschool_dissertations/5880)



- Mostafiz, R.B., Assi, A.A., Friedland, C., Rohli, R., & Rahim, M.A. (2022d). A Numerically-integrated Approach for Residential Flood Loss Estimation at the Community Level. In EGU General Assembly 2022. Vienna, Austria, 23–27 May. <https://doi.org/10.5194/egusphere-egu22-10827>
- Mukherjee, S., Nateghi, R., & Hastak, M. (2018). A multi-hazard approach to assess severe weather-induced major power outage risks in the U.S. *Reliability Engineering & System Safety*, 175, 283–305. doi:10.1016/j.ress.2018.03.015
- National Oceanic and Atmospheric Administration. National Centers for Environmental Information. Global Historical Climate Network Daily. (2017a). <https://www.ncdc.noaa.gov/ghcn-daily-description> [Accessed February 11, 2021].
- National Oceanic and Atmospheric Administration, National Centers for Environmental Information. (2017b). <https://www.ncei.noaa.gov/> [Accessed February 11, 2021].
- National Oceanic and Atmospheric Administration, National Centers for Environmental Information. (2018). *Storm Data Preparation*. Operations and Services Performance, NWSPD 10-16. <https://www.nws.noaa.gov/directives/sym/pd01016005curr.pdf>, p. 14 [Accessed February 11, 2021].
- National Oceanic and Atmospheric Administration. National Centers for Environmental Information. U.S. Billion-Dollar Weather and Climate Disasters (2020). <https://www.ncdc.noaa.gov/billions/> doi:10.25921/stkw-7w73
- National Oceanic and Atmospheric Administration. National Severe Storms Laboratory. (2014). <https://www.nssl.noaa.gov/> [Accessed February 11, 2021].
- Paul, S. H., & Sharif, H. O. (2018). Analysis of damage caused by hydrometeorological disasters in Texas, 1960–2016. *Geosciences* 8(10), Art. No.: UNSP 384. doi:10.3390/geosciences8100384.
- Peña-Gallardo, M., Vicente-Serrano, S. M., Quiring, S., Svoboda, M., Hannaford, J., Tomas-Burguera, M., Martín-Hernández, N., Domínguez-Castro, F., & El Kenawy, A. (2019). Response of crop yield to different time-scales of drought in the United States: Spatio-temporal patterns and climatic and environmental drivers. *Agricultural and Forest Meteorology*, 264(2019), 40–55. doi:10.1016/j.agrformet.2018.09.019
- Pielke Sr, R. A., Adegoke, J., Beltrán-Przekurat, A., Hiemstra, C. A., Lin, J., Nair, U. S., Niyogi, D., & Nobis, T. E. (2007). An overview of regional land-use and land-cover impacts on rainfall. *Tellus B: Chemical and Physical Meteorology*, 59(3), 587–601. doi:10.1111/j.1600-0889.2007.00251.x
- Potopova, V., Boroneanț, C., Boincean, B., & Soukup, J. (2016). Impact of agricultural drought on main crop yields in the Republic of Moldova. *International Journal of Climatology*, 36(4), 2063–2082. doi:10.1002/joc.4481
- Preston, B. L. (2013). Local path dependence of U.S. socioeconomic exposure to climate extremes and the vulnerability commitment. *Global Environmental Change*, 23(4), 719–732. doi:10.1016/j.gloenvcha.2013.02.009
- Púčik, T., Castellano, C., Groenemeijer, P., Kühne, T., Rädler, A. T., Antonescu, B., & Faust, E. (2019). Large hail incidence and its economic and societal impacts across Europe. *Monthly Weather Review*, 147(11), 3901–3916. doi:10.1175/MWR-D-19-0204.1

- Rahim, M.A., Gnan, E.S., Friedland, C.J., Mostafiz, R.B., & Rohli, R.V. (2022). *An Improved Micro Scale Average Annual Flood Loss Implementation Approach*. In EGU General Assembly 2022. Vienna, Austria, 23–27 May. <https://doi.org/10.5194/egusphere-egu22-10940>
- Rahman, M.A., & Rahman, S. (2015). Natural and traditional defense mechanisms to reduce climate risks in coastal zones of Bangladesh. *Weather and Climate Extremes*, 7, 84–95. doi:10.1016/j.wace.2014.12.004.
- Refan, M., Romanic, D., Parvu, D., & Michel, G. (2020). Tornado loss model of Oklahoma and Kansas, United States, based on the historical tornado data and Monte Carlo simulation. *International Journal of Disaster Risk Reduction*, 43, 101369. doi:10.1016/j.ijdrr.2019.101369
- Reinhold, T. A., & Ellingwood, B. (1982). *Tornado Damage Risk Assessment* (No. NUREG/CR--2944). National Bureau of Standards.
- Rohli, R. V., Bushra, N., Lam, N., Zou, L., Mihunov, V. Reams, M.A., & Argote, J. E. (2016). Drought indices as drought predictors in the south-central United States. *Natural Hazards* 83(3), 1567–1582. doi:10.1007/s11069-016-2376-z.
- Smith, A. B., & Katz, R. W. (2013). US billion-dollar weather and climate disasters: Data sources, trends, accuracy and biases. *Natural Hazards*, 67(2013), 387–410. doi:10.1007/s11069-013-0566-5
- Smith, A. B., & Matthews, J. L. (2015). Quantifying uncertainty and variable sensitivity within the US billion-dollar weather and climate disaster cost estimates. *Natural Hazards*, 77(3), 1829–1851. doi:10.1007/s11069-015-1678-x
- Storm Prediction Center. (2017). National Oceanic and Atmospheric Administration. <https://www.spc.noaa.gov/> [Accessed February 11, 2021].
- United States Census Bureau. (2016). TIGER/Line Shapefiles. **Error! Hyperlink reference not valid.** <https://www.census.gov/geographies/mapping-files/time-series/geo/tiger-line-file.html> [Accessed February 11, 2021].
- United States Census Bureau. (2020). Census Bureau Releases International Population Estimates and Projections, International data base web tool. **Error! Hyperlink reference not valid.** [https://www.census.gov/data-tools/demo/idb/#/country?YR\\_ANIM=2020](https://www.census.gov/data-tools/demo/idb/#/country?YR_ANIM=2020) [Accessed February 11, 2021].
- United States Department of Agriculture (USDA) Economic Research Service. (2017). <https://www.ers.usda.gov/data-products/state-export-data/annual-state-agricultural-exports/> [Accessed February 11, 2021].
- United States Department of Agriculture (USDA) National Agricultural Statistics Service. (2020). <https://www.nass.usda.gov/> [Accessed February 11, 2021].
- United States Drought Monitor. (2017). National Oceanic and Atmospheric Administration. <https://droughtmonitor.unl.edu/> [Accessed February 11, 2021].
- United States Drought Portal. (2020). National Integrated Drought Information System. <https://www.drought.gov/drought/states/louisiana#:~:text=from%202000%20%2D%202020,affect%2064.94%25%20of%20Louisiana%20land> [Accessed February 11, 2021].
- United States Global Change Research Program. (2017). Climate Science Special Report: Fourth National Climate Assessment, Volume I. eds. Wuebbles, D. J., Fahey, D. W., Hibbard, K. A.,

- 882       Dokken, D. J., Stewart, B. C., & Maycock, T. K. U.S. Global Change Research Program,  
883       Washington, D.C., USA, 470. doi:10.7930/J0J964J6.
- 884       United States Geological Survey (USGS). (2016).  
885       [https://www.usgs.gov/centers/eros/science/national-land-cover-database?qt-](https://www.usgs.gov/centers/eros/science/national-land-cover-database?qt-science_center_objects=0#qt-science_center_objects)  
886       [science\\_center\\_objects=0#qt-science\\_center\\_objects](https://www.usgs.gov/centers/eros/science/national-land-cover-database?qt-science_center_objects=0#qt-science_center_objects) [Accessed February 11, 2021].
- 887       University of Arkansas Division of Agriculture. (2021). Economic impact of agriculture.  
888       <https://economic-impact-of-ag.uark.edu/louisiana/> [Accessed February 11, 2021].
- 889       Villamil, D. E., Santamaria, F., & Diaz, W. (2015). Lightning disaster risk assessment method in  
890       Colombia. In *2015 International Symposium on Lightning Protection (XIII SIPDA)* 146–152.  
891       IEEE.
- 892       Vose, R. S., Easterling, D. R., Kunkel, K. E., LeGrande, A. N., & Wehner, M. F. (2017).  
893       Temperature changes in the United States. In *Climate Science Special Report: Fourth*  
894       *National Climate Assessment, Volume I*, eds. D. J. Wuebbles, D. W. Fahey, K. A. Hibbard, D.  
895       J. Dokken, B. C. Stewart, & T. K. Maycock (Washington D.C.: U.S. Global Change Research  
896       Program), 185–206. doi:10.7930/J0N29V45.
- 897       Wang, L., Hu, G., Yue, Y., Ye, X., Li, M., Zhao, J., & Wan, J. (2016). GIS-based risk assessment of  
898       hail disasters affecting cotton and its spatiotemporal evolution in China. *Sustainability*, 8(3),  
899       218. doi:10.3390/su8030218
- 900       Wehner, M. F., J. R. Arnold, T. Knutson, K. E. Kunkel, & A. N. LeGrande. 2017. Droughts, floods,  
901       and wildfires. In: *Climate Science Special Report: Fourth National Climate Assessment,*  
902       *Volume I* [Wuebbles, D. J., Fahey, D. W., Hibbard, K. A., Dokken, D. J., Stewart, B. C., &  
903       Maycock, T. K. (eds.)]. U.S. Global Change Research Program, Washington, DC, USA, pp.  
904       231–256. doi:10.7930/JOCJ8BNN
- 905       Wilhite, D. A. (2000). Chapter 1 Drought as a Natural Hazard: Concepts and Definitions. Drought  
906       Mitigation Center Faculty Publications. 69.  
907       [https://digitalcommons.unl.edu/droughtfacpub/69/?utm\\_source=digitalcommons.unl.edu%2F](https://digitalcommons.unl.edu/droughtfacpub/69/?utm_source=digitalcommons.unl.edu%2Fdroughtfacpub%2F69&utm_medium=PDF&utm_campaign=PDFCoverPages)  
908       [droughtfacpub%2F69&utm\\_medium=PDF&utm\\_campaign=PDFCoverPages](https://digitalcommons.unl.edu/droughtfacpub/69/?utm_source=digitalcommons.unl.edu%2Fdroughtfacpub%2F69&utm_medium=PDF&utm_campaign=PDFCoverPages) [Accessed  
909       November 23, 2021].
- 910       Wu, J. D., Y. Li, N. Li, & P. J. Shi. 2018. Development of an asset value map for disaster risk  
911       assessment in China by spatial disaggregation using ancillary remote sensing data. *Risk*  
912       *Analysis*, 38(1), 17–30. doi:10.1111/risa.12806
- 913       Zhang, X., & Hu, H. (2018). Copula-based hazard risk assessment of winter extreme cold events in  
914       Beijing. *Atmosphere*, 9(7), 263. doi:10.3390/atmos9070263
- 915       Zhang, W., Meng, Q., Ma, M., & Zhang, Y. (2011). Lightning casualties and damages in China from  
916       1997 to 2009. *Natural Hazards*, 57(2), 465–476. doi:10.3390/atmos9070263
- 917       Zhou, J., Pavek, M. J., Shelton, S. C., Holden, Z. J., & Sankaran, S. (2016). Aerial multispectral  
918       imaging for crop hail damage assessment in potato. *Computers and Electronics in*  
919       *Agriculture*, 127, 406–412. doi:10.1016/j.compag.2016.06.019
- 920       Zscheischler, J., Westra, S., van den Hurk, B. J. J. M., Seneviratne, S. I., Ward, P. J., Pitman, A.,  
921       AghaKouchak, A., Bresch, D. N., Leonard, M., Wahl, T., & Zhang, X. (2018). Future climate  
922       risk from compound events. *Nature Climate Change*, 8(6), 469–477. doi:10.1038/s41558-  
923       018-0156-3.